



# Magnetic Properties and Crystallization of the Fe<sub>75</sub>Si<sub>15</sub>B<sub>10</sub> Amorphous Alloy Prepared by Mechanical Alloying

J. QUISPE MARCATOMA<sup>1</sup>, V. A. PEÑA RODRÍGUEZ<sup>1</sup> and E. M. BAGGIO-SAITOVITCH<sup>2</sup>

<sup>1</sup>*Facultad de Ciencias Físicas, Universidad Nacional Mayor de San Marcos, P.O. Box 14-0149, Lima 14, Perú*

<sup>2</sup>*Centro Brasileiro de Pesquisas Físicas, Rua Dr. Xavier Sigaud 150, Urca, CEP 22290-180, Rio de Janeiro, Brazil*

**Abstract.** The magnetic order and crystallization of the amorphous Fe<sub>75</sub>Si<sub>15</sub>B<sub>10</sub> alloy prepared by mechanical alloying was studied *in situ* by <sup>57</sup>Fe Mössbauer spectroscopy. These measurements were carried out using a vacuum furnace, controlling the temperature in the absorber. From Mössbauer measurements the magnetic order temperature of the as-milled sample was estimated at about 675 K. In order to identify the crystalline phases formed during heating, Mössbauer measurements were analyzed together with X-ray diffraction analysis. Both results show the formation of several crystalline phases such as Fe<sub>5</sub>SiB<sub>2</sub>, Fe<sub>2</sub>B, Fe<sub>3</sub>Si,  $\alpha$ -Fe, Fe–B composite and a residual amorphous phase.

**Key words:** mechanical alloying, metallic alloys, soft magnetic materials, Mössbauer spectroscopy.

## 1. Introduction

FeSiB-based alloys produced by melt-spun technique have been submitted to intense scientific investigation over the past two decades due to their excellent soft magnetic properties. It is well known that these alloys are used in several applications, including power devices, information handling and magnetic sensors [1, 2]. The crystallization process of Fe–Si–B alloys has been studied using different methods [3, 4]. In particular, Illeková *et al.* [5] and Mat'ko *et al.* [6] investigated the crystallization of glassy Fe<sub>75</sub>Si<sub>15</sub>B<sub>10</sub> using DSC. However, as far as we know, Mössbauer spectroscopy measurements have not been reported.

Illeková and Mat'ko found that this amorphous alloy exhibits a Curie temperature ( $T_C$ ) at 707 K and a double exothermic crystallization peak at 817 K and 830 K ( $\varphi = 10 \text{ K min}^{-1}$ ). The first peak was attributed to the crystallization of two types of microcrystals namely  $\alpha$ -Fe(Si), Fe<sub>3</sub>Si and a composite crystal containing cores of Fe<sub>3</sub>B with  $\alpha$ -Fe(Si) growing on the surface. The second peak was attributed mainly to the transformation of the metastable Fe<sub>3</sub>B to Fe<sub>2</sub>B and  $\alpha$ -Fe.

Recently, some efforts have been made to obtain amorphous Fe–B–Si powders using the ball-milling technique; however, they were able to produce a crys-

talline solid solution [7] or only partial formation of the amorphous phase [8]. The work described here is part of a research about the synthesis and crystallization of  $\text{Fe}_{75}\text{Si}_{15}\text{B}_{10}$  amorphous powder prepared by mechanical alloying [9].

## 2. Experimental

$\text{Fe}_{75}\text{Si}_{15}\text{B}_{10}$ (at%) powder alloys were prepared by mechanical alloying from a mixture of pure elemental powders [9]. The powders were sealed in a round-ended SPEX mill container with stainless-steel ball in an argon atmosphere and they processed using a mixer mill SPEX 8000 unit. A ball-to-powder weight ratio 8 : 1 was used. During the process, small quantities of powder were removed in order to examine the evolution of structure and microstructure from the starting materials and after 19 h of ball milling a homogeneous amorphous fraction was obtained. An *in situ* Mössbauer study of the crystallization was performed using a vacuum furnace ( $\sim 10^{-6}$  mbar), controlling the absorber temperature in the range 300–800 K. These measurements were carried out employing a heating rate  $\varphi$  of  $0.2 \text{ K min}^{-1}$  where each spectrum was recorded during 3 h. During these measurements, a 25 mCi  $^{57}\text{Co/Rh}$  radioactive source was used keeping the source at room temperature. In order to identify the phases formed during crystallization, a dynamic thermal treatment was performed on the as-prepared samples with a heating rate,  $\varphi = 5 \text{ K min}^{-1}$  under Ar atmosphere. X-ray diffraction measurements were performed on these crystallized samples by using  $\text{Cu-K}\alpha_1$  radiation in a Rigaku RU-200B diffractometer, implemented with a graphite monochromator.

## 3. Results and discussion

Figure 1 shows the temperature dependence of the *in situ* Mössbauer spectra obtained during the heating process. At the bottom and at the top of the figure are displayed the spectra recorded at 300 K from the as-milled initial sample and the crystallized end-sample, respectively.

From Figure 1 a broad six-line pattern is observed up to 450 K, which is associated to magnetic order present on the sample. At temperatures beyond 450 K, the two central lines become increasingly important and above 650 K the six-line pattern collapses onto a paramagnetic doublet. The Mössbauer spectra were fitted using one discrete distribution of hyperfine magnetic fields. The unusual increase of the two central lines reveals that the temperature dependence of our Mössbauer spectra is significantly different from the common thermal behavior showed on the of FeSiB-based amorphous alloys [10–12], where the six-line absorption pattern collapses progressively while the temperature rises.

Figure 2 shows the temperature dependence of the magnetic hyperfine field distribution  $P(B_{\text{hf}})$  taken between 4.2 K and 650 K. It is important to note that within the current procedure the main peaks of the  $P(B_{\text{hf}})$  shift to lower values while the temperature rises. In addition, the presence of two humps in the distributions up

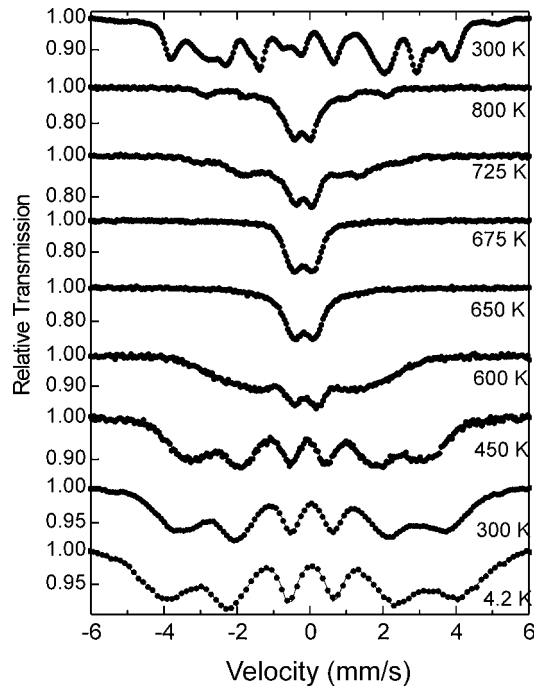


Figure 1. Temperature dependence of the Mössbauer spectra for the  $\text{Fe}_{75}\text{Si}_{15}\text{B}_{10}$  alloys obtained during the heating process. Note the signal of some magnetic lines at 725 and 800 K.

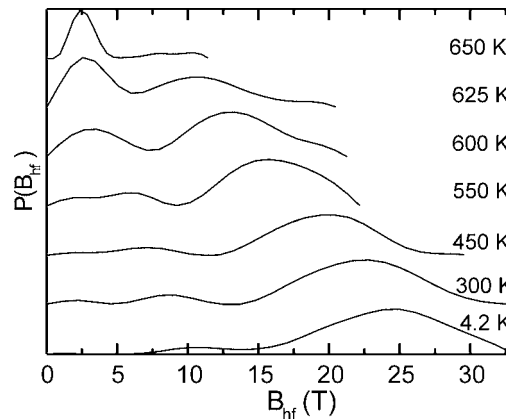


Figure 2. Evolution of the hyperfine field distributions  $P(B_{\text{hf}})$  in the range 4.2–650 K.

to 450 K could be mainly associated to two different iron environments. However, at temperatures beyond 450 K, the variance of the whole distribution increases, which indicates that all components of  $P(B_{\text{hf}})$  do not have the same temperature dependence. From Figure 3 it is observed that the average magnetic field decreases as the temperature increases, resulting in a magnetic order temperature of around 675 K.

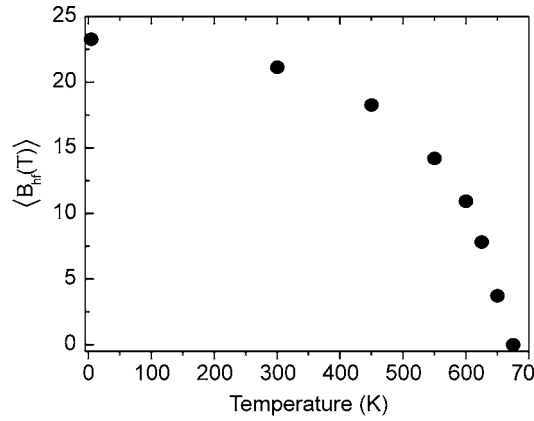


Figure 3. Temperature dependence of  $\langle B_{\text{hf}} \rangle$  in the temperature range 4.2–650 K.

Table I. Room-temperature Mössbauer hyperfine parameters of the crystallized sample. Isomer shifts are given relative to  $\alpha$ -Fe

		$B_{\text{hf}}$ (T)	$\delta$ (mm/s)	ARE (%)
$\text{Fe}_2\text{B}$	site A	24.24(1)	0.137(1)	14
	site B	23.37(1)	0.1083	15
$\text{Fe}_5\text{SiB}_2$	site (1) A	17.843(6)	0.2754(6)	21
	site (2)	23.47(1)	0.160	7
$\text{Fe}_3\text{Si}$	site D	31.613	0.0775	2
	site A	20.053(7)	0.268(8)	15
Composite FeB		16.578(7)	0.3077(9)	15
$\alpha$ -Fe		32.8	-0.036	1
Amorphous residual		8.94(1)	0.197(1)	10

Our results show that the disappearance of the magnetic order occurs progressively for  $T > 450$  K. This fact suggests a coexistence of paramagnetic and magnetic contributions, probably due to a gradual crumbling of the magnetic order into small superparamagnetic clusters as the critical temperature is approached from below [13].

Following the annealing process, for the temperature range  $675 \text{ K} < T < 700 \text{ K}$ , Mössbauer spectra were fitted using one quadrupole paramagnetic doublet. At temperatures above 725 K Mössbauer spectra show a complex profile as a consequence of the crystallization process of the glassy sample. These spectra were fitted using several components. One paramagnetic doublet, associated to a residual amorphous phase in paramagnetic state, and some sextets attributed to the formation of several crystalline phases. These crystalline components were identified as  $\text{Fe}_2\text{B}$  [14],

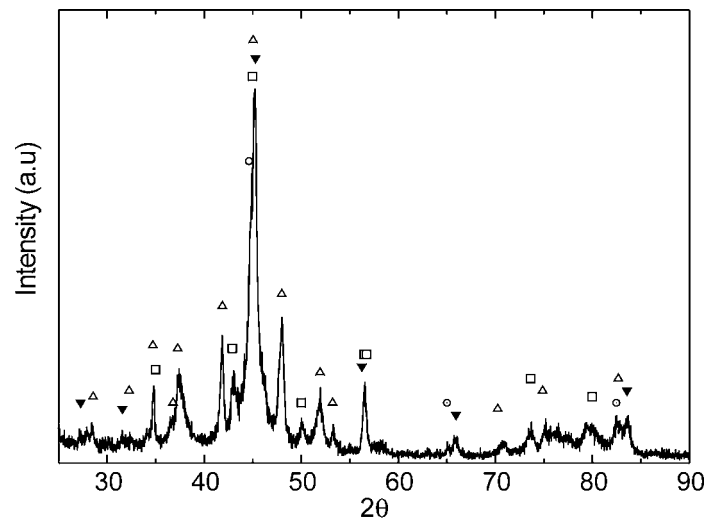


Figure 4. X-ray diffraction pattern after annealing of the  $\text{Fe}_{75}\text{Si}_{15}\text{B}_{10}$  alloys obtained by mechanical alloying. (□)  $\text{Fe}_2\text{B}$ , (Δ)  $\text{Fe}_5\text{SiB}_2$ , (▼)  $\text{Fe}_3\text{Si}$ , and (○)  $\alpha\text{-Fe(Si)}$ .

$\text{Fe}_5\text{SiB}_2$  [15],  $\text{Fe}_3\text{Si}$  [16],  $\alpha\text{-Fe}$  and  $\text{Fe-B}$  composite. The Mössbauer hyperfine parameters corresponding to the crystallized sample recorded at room temperature are shown in Table I.

Figure 4 shows the diffraction peaks corresponding to the crystallized sample. These results show the presence of  $\text{Fe}_5\text{SiB}_2$ ,  $\text{Fe}_2\text{B}$ ,  $\text{Fe}_3\text{Si}$  and  $\alpha\text{-Fe(Si)}$  and agree with those obtained by Mössbauer spectroscopy.

#### 4. Conclusions

Our results show that the temperature dependence of Mössbauer spectra of  $\text{Fe}_{75}\text{Si}_{15}\text{B}_{10}$  amorphous powder alloys prepared by mechanical alloying is very different from the amorphous state obtained by melt spun technique. These differences may be associated to the fact that our sample is not completely amorphous, which might be formed by several Fe nanocrystalline [9] components attributed to the  $\text{Fe}_2\text{B}$ ,  $\text{Fe}_5\text{SiB}_2$ ,  $\text{Fe}_3\text{Si}$ ,  $\alpha\text{-Fe}$  and  $\text{FeB}$  composite crystal.

#### Acknowledgements

The authors would like to acknowledge the financial support provided by CSI-UNMSM under project N° 011301021, FAPERJ-Brazil (Cientista do Nosso Estado) and Latin American Center of Physics. It is a pleasure to thank Prof. J. M. Greneche for his helpful contribution.

## References

1. Graham, C. D. and Egami, T., *J. Magn. Magn. Mater.* **15–18** (1980), 1325.
2. Meydan, T., *J. Magn. Magn. Mater.* **133** (1994), 525.
3. Ramanan, V. R. V. and Fish, G. E., *J. Appl. Phys.* **53** (1982), 2273.
4. Gibson, M. A. and Delamore, G. W., *Acta Metall. Mater.* **38** (1990), 2621.
5. Illeková, E., Mat'ko, I., Duhaj, P. and Kuhnast, F., *J. Mater. Sci. Eng.* **32** (1997), 4645.
6. Illeková, E., Švec, P., Duhaj, P. and Mat'ko, I., *Mater. Sci. Eng. A* **225** (1997), 145.
7. Jachimowicz, M., Fadeeva, V. I., Matyja, H. and Grabias, A., *Mater. Sci. Forum* **360–362** (2001), 537.
8. Suriñach, S., Baró, M. D., Segura, J. and Clavaguera-Mora, M. T., *Mater. Sci. Eng. A* **134** (1991), 1368; Kunitomi, N., *Mat. Sci. Eng. A* **181–182** (1994), 1296.
9. Quispe Marcatoma, J. and Peña Rodríguez, V. A., *Hyp. Interact.* **134** (2001), 207.
10. Shurer, P. J. and Morrish, A. H., *Phys. Rev. B* **20** (1979), 4660.
11. Bhatnagar, A. K., Prasad, B. B. and Jagannathan, R., *Phys. Rev. B.* **29** (1984), 4896.
12. Banerji, N., Johri, U. C., Kulkarni, V. N. and Singru, R. M., *J. Mater. Sci.* **30** (1995), 417.
13. Grenéche, J. M., *J. Non-Cryst. Sol.* **287** (2001), 37.
14. Takacs, L., Cadeville, M. C. and Vincze, I., *J. Phys. F* **5** (1975), 800; Vincze, I., Kemeny, T. and Arajs, S., *Phys. Rev. B* **21** (1980), 937.
15. Ericsson, T., Häggström, L. and Wäppling, R., *P. Script.* **17** (1978), 83.
16. Stearns, M. B., *Phys. Rev.* **129** (1963), 1136.